Published in final edited form as:
Cancer Res. 2012 April 1; 72(7): 1717–1727. doi:10.1158/0008-5472.CAN-11-3758.

Cancer vaccination drives Nanog-dependent evolution of tumor cells towards an immune-resistant and stem-like phenotype

Kyung Hee Noh[1], **Young-Ho Lee**[1], **Ju-Hong Jeon**[2], **Tae Heung Kang**[3], **Chih-Ping Mao**[3], **T-C Wu**[3,4,5,6], and **Tae Woo Kim**[1]

[1]Divison of Infection and Immunology, Graduate School of Medicine, Korea University, Seoul, South Korea

[2]Department of Physiology, Seoul National University, College of Medicine, Seoul, South Korea

[3]Department of Pathology, Johns Hopkins School of Medicine, Baltimore, MD, USA

[4]Department of Obstetrics and Gynecology, Johns Hopkins School of Medicine, Baltimore, MD, USA

[5]Department of Oncology, Johns Hopkins School of Medicine, Baltimore, MD, USA

[6]Department of Molecular Microbiology and Immunology, Johns Hopkins School of Medicine, Baltimore, MD, USA

Abstract

Due to the exquisite specificity and potency of the immune system, vaccination is in theory the most precise and powerful approach for controlling cancer. However, current data from clinical trials indicate that vaccination rarely yields significant benefits for cancer patients in terms of tumor progression and long-term survival. The poor clinical outcomes of vaccination are primarily caused by mechanisms of immune tolerance, especially within the tumor microenvironment. Here we report that vaccination drives the evolution of tumor cells towards an immune-resistant and stem-like phenotype that promotes tumor growth and nullifies the cytotoxic T lymphocyte (CTL) response. The emergence of this phenotype required the transcription factor Nanog, which is induced as a consequence of immune selection. Nanog expression enhanced the stem-like features of tumor cells and protected them from killing by tumor-reactive CTLs. Delivery of siNanog into tumor-bearing mice rendered the tumor vulnerable to immune surveillance and strongly suppressed its growth. Together, our findings demonstrate tumor adaptation to vaccination through gain of an immune-resistant, stem-like phenotype and identify Nanog as a central molecular target in this process. Future vaccination technology should consider Nanog an important target to enhance the immunotherapeutic response.

Keywords

Cancer stem cell; immune escape; vaccination; human papillomavirus (HPV)

Corresponding authors: T-C Wu, Department of Pathology, Johns Hopkins School of Medicine, CRB II Room 309, 1550 Orleans Street, Baltimore, MD 21231, USA. Phone: (410) 614-3899; fax: (443) 287-4295; wutc@jhmi.edu. Tae Woo Kim, Division of Infection and Immunology, Graduate School of Medicine, Korea University, 516 Gojan-1 Dong, Ansan-Si, Gyeonggi-Do 425-707, Seoul, South Korea. Phone: +82-31-412-6713; fax: +82-31-412-6718; twkim0421@korea.com.

Introduction

The establishment of tumor-reactive $CD8^+$ CTLs by vaccination represents a potentially effective route for the management of cancer. CTLs have unequivocal specificity and potency to destroy transformed cells throughout the body without inflicting significant damage to normal tissue (1, 2). Generation of immune memory after tumor eradication should also protect against long-term relapse (3, 4). These advantages of vaccination over conventional cancer treatments fueled much of the enthusiasm for vaccination in the early 21^{st} century (5, 6). However, this enthusiasm has gradually waned due to poor clinical outcomes, even after aggressive vaccination regimens (7–10).

These results from early clinical trials persuaded investigators to elucidate mechanisms responsible for the failure of vaccination. Multiple strategies are being studied to overcome hurdles of the immunosuppressive tumor milieu (11). However, tumor cells themselves may adapt to selection pressures imposed by vaccination, making them impervious to immune surveillance. Here we show that vaccination induces tumor cells to express Nanog, a homeobox transcription factor pivotal in self-renewal of embryonic stem cells. Nanog confers tumor cells with an immune-resistant and stem-like phenotype, thereby facilitating tumor progression. Knockdown of Nanog expression with small interfering RNA (siRNA) renders the tumor vulnerable to immune attack and leads to reduction in tumor growth. We also show that Nanog is present in some human cancer cells and that it promotes immune escape and stem-like features in this setting. Our data suggest that Nanog-dependent evolution of tumor cells towards an immune-resistant and stem-like phenotype poses a critical, previously unrecognized obstacle to vaccination. Inhibition of Nanog provides an avenue to overcome this obstacle and may help realize the clinical promise of cancer vaccination.

Materials and methods

Mice

6- to 8-week old female C57BL/6 and NOD/SCID mice (Central Lab Animal Inc., Seoul, Korea) were maintained and handled under protocol approved by the Korea University Institutional Animal Care and Use Committee (KUIACUC-2009-126).

DNA constructs

To generate pMSCV/Nanog, DNA fragments encoding Nanog were amplified from pSIN-EF2-Nanog-Pur-expressing cells (Addgene, Cambridge, MA) using the primer set: 5' – GCCTCGAGATGAGTGTGGATCCAGCTTG – 3' and 5 ' – GCGAATTCTCACACGTCTTGAGGTTG – 3'. Amplified DNA was cloned into the XhoII/EcoRI sites of the pMSCV retroviral vector (Clontech, CA). Plasmid integrity was verified by DNA sequencing.

siRNA constructs and delivery

siRNA specific for green fluorescent protein (GFP), mouse Nanog (mNanog), or human Nanog (hNanog) (Invitrogen, CA) contained the sequences: GFP, 5'–GCAUCAAGGUGAACUUCAA – 3', 5' – UUGAAGUUCACCUUGAUGC – 3'; mNanog, 5' – GUUAAGACCUGGUUUCAAA – 3', 5' – UUUGAAACCAGGUCUUAAC – 3'; hNanog, 5' – GCAACCAGACCUGGAACAAUU – 3', 5' – UUGUUCCAGGUCUGGUUGCUU – 3'. For *in vitro* siRNA delivery, cells were plated in 6-well reaction vessels and transfected by Lipofectamine 2000 (Invitrogen) with 300 pmol of siRNA. For systemic *in vivo* siRNA delivery, chitosan nanoparticles were prepared as previously described (12).

Cells

TC-1 P0 and P3 cells were produced in our laboratory and maintained as previously described (13). HEK293, HeLa, CaSki, and CUMC6 cells were from American Type Culture Collection (ATCC, VA). TC-1/empty, TC-1/Nanog, HEK293-D^b/empty, HEK293-D^b/Nanog, CaSki/empty, and CaSki/Nanog cells were generated by retroviral transduction with pMSCV/empty, pMSCV/D^b, pMSCV/mNanog, or pMSCV/hNanog, and, after puromycin selection (0.5μg/ml), the transduced cells were cultured with 0.25 μg/ml of puromycine. HEK293, HEK293-D^b/empty, HEK293-D^b/Nanog cells were grown in DMEM with 10% v/v fetal bovine serum (FBS), 50 units/ml penicillin/streptomycin, 2 mM L-glutamine, 1 mM sodium pyruvate, and 2 mM non-essential amino acids, and the other cells in RPMI 1640 with 2 mM L-glutamine adjusted to contain 1.5 g/L sodium bicarbonate, 4.5 g/L glucose, 10 mM HEPES, 1.0 mM sodium pyruvate supplemented with 0.1 mM nonessential amino acids at 37°C in a 5% CO_2 incubator.

Tumor sphere-forming assays

Cells were plated at 5×10^3 cells per well in ultra low attachment vessels (Corning, MA) containing serum-free DMEM/F12 (Thermo Scientific, MA), supplemented with epidermal growth factor (20 ng/ml), basic fibroblast growth factor (10 ng/ml), and B27 (Invitrogen). Medium was replaced every 3 days to replenish growth factors and nutrients.

Tumorigenicity assay

TC-1 P0 or P3 cells were harvested by trypsinization, washed with Opti-MEM (Invitrogen), and resuspended in Opti-MEM. NOD/SCID mice were subcutaneously injected with 1×10^2, 1×10^3, or 1×10^4 TC-1 P0 or P3 cells. Tumor formation was monitored at least 3 times per week. After 18 days, tumor tissue was excised and weighed.

Real-time quantitative RT-PCR

Total RNA from TC-1 cells was purified using TRIzol reagent (Invitrogen). First-strand synthesis and real-time PCR were performed to detect mNanog with TaqMan Universal SYBR Green Master Mix (Roche, IN) using the primer set: 5' – ATGAGTGTGGATCCAGCTTG – 3' (forward), 5' – TCACACGTCTTGAGGTTG – 3' (reverse).

Immunofluorescence microscopy

TC-1 cells were fixed in 4% paraformaldehyde for 10 minutes. After washing with PBS, cells were treated with 0.2% Triton X-100 and blocked for 1 hour in 1% BSA solution. Primary antibodies against Nanog or Oct4 (Santa Cruz Biotechnology, CA) were added for overnight incubation in a humidified chamber at 4°C. Cells were stained with Alexa Flour 488-labeled goat anti-mouse IgG and DAPI. Expression of Nanog and Oct4 was analyzed by confocal laser scanning microscopy (Carl Zeiss, Oberkochen, Germany) as previously described (14).

Western blot

A total of 5×10^5 cells was used to perform Western blot as previously described (15). Primary antibodies against CDK2, cyclin E, cyclin A (Cell Signaling Technology, MA), Nanog, Oct4, Sox2, c-Myc, p21, and p27 (Santa Cruz Biotechnology), Nestin (BD Biosciences, CA), ALDH3A1, and Musanshi1 (Abcam, CA) were used at 1:1000 dilution. Immune-reactive bands were visualized by enhanced chemiluminescence (Elpis Biotech, Daejeon, Korea).

Flow cytometry

For CTL assays, siGFP- or siNanog-transfected TC-1 P3 cells, TC-1/empty cells, or TC-1/Nanog cells were mixed with E7-specific CTLs at a 1:1 effector:target ratio for 4 hours. Surface staining for CD8 and intracellular staining for IFN-γ followed by flow cytometry were performed as previously described (16). For cell cycle analysis, the cells were resuspended in PBS containing 0.2 μg/μl propidium iodide and incubated for 30 minutes after cold ethanol fixation. All data acquisition was performed on a FACSCalibur flow cytometer (BD Biosciences) with CellQuest Pro software.

Granzyme B apoptosis assays

Human granzyme B (GrB) (Enzo Life Sciences, NY) was delivered into cells with the BioPORTER QuikEase protein delivery kit (Sigma-Aldrich, MO). 5×10^4 cells were plated into a 24-well reaction vessel and cultured overnight at 37°C. Cells were then washed with Opti-MEM, and 200 ng of GrB in Opti-MEM was added to each well. After a 4 hour incubation at 37°C, frequency of apoptotic cells was determined with anti-active caspase 3 antibody as previously described (15).

Tumor treatment experiments

To characterize the *in vivo* resistance to CTL lysis conferred by Nanog, C57BL/6 mice were subcutaneously injected with 1×10^5 TC-1/empty or TC-1/Nanog cells in the left hind leg. After 3 days, mice received adoptive transfer with either 2×10^6 E7-specific CTLs or isotonic saline. Tumor size was measured for 10 days following tumor challenge. To evaluate the therapeutic effect of Nanog inhibition, mice were subcutaneously injected with 1×10^5 TC-1 P3 cells in the left hind leg. siRNA nanoparticles targeting either GFP or mNanog (5 μg/animal) were injected intravenously 6, 7, and 8 days after tumor challenge. After 9 days, mice received adoptive transfer with 2×10^6 E7-specific CTLs. Tumor size was measured for the next 15 days.

Statistical analysis

All data are representative of at least three independent experiments. Non-parametric 1-way or 2-way ANOVA was performed with SPSS version 12.0 software (IBM, IL). Comparisons between individual data points were assessed with Student's T-test. A p-value of $p<0.05$ was considered significant in all cases.

Results

Vaccination enhances growth and stem-like properties of tumor cells

According to the cancer immunoediting theory, heterogeneous tumor cells are continuously subjected to host immune surveillance (17, 18). Cells vulnerable to immune surveillance are eliminated, while cells that evade detection and killing proliferate. A corollary of this theory is that vaccination should accelerate and intensify the selection of these escape variants. We previously devised a system —coined here as vaccination-induced cancer evolution (VICE) —to simulate immunoediting in the context of vaccination (19). We applied VICE to generate immune-resistant tumor cells in a human papillomavirus (HPV) type-16-associated cervical cancer model, TC-1, which allows us to accurately trace tumor-reactive CTLs based on specificity for the HPV antigen E7 (13). After 3 serial passages, we created TC-1 P3, a derivative of the parental TC-1 line (P0), that is completely impervious to Sig/E7/LAMP-1-based vaccination (19–21).

Since cancer stem cells (CSCs) — cells critical for tumor initiation and maintenance — have the capacity to survive and thrive despite chemotherapy or radiotherapy (22, 23), we asked

whether vaccination could enhance the stem-like properties of tumor cells, in addition to the immune-resistant phenotype. To address this question, we first characterized the growth of TC-1 P0 and P3 cells. Compared to P0 cells, P3 cells divided 3 times more rapidly (Figure 1A), contained a higher proportion of cells in S phase (Figure 1B), had elevated cyclin A expression, and decreased cyclin-dependent kinase inhibitor p21 expression (Figure 1C). These data show that P3 cells have greater proliferative capacity than P0 cells. We next explored the stem-like properties of P3 cells. CSCs tend to form spheres when cultured in low-attachment vessels under serum-depleted conditions. In these conditions, P3 cells produced more spheres than P0 cells (Figure 1D), and these spheres could be continuously passaged (Figure 1E). P3 cells also had increased expression of stemness markers CD133, CD44, and aldehyde dehydrogenase (ALDH) (Supplemental Figure 1A). CSCs can also give rise to tumors in immunocompromised mice. We inoculated NOD/SCID mice with 10^2 to 10^4 P0 or P3 cells and assessed tumor formation. Challenge with 10^3 P0 cells did not produce tumors in any of the mice, but just 10^2 P3 cells produced tumors in 80% of the mice (Figure 1F). Challenge with 10^4 P0 or P3 cells produced tumors in 60% or 100% of the mice, respectively (Figure 1F), but the tumor was nearly 10 times larger in the P3-challenged mice relative to the P0-challenged mice (Figure 1G). Based on these results, the P3 line is over 100-fold more tumorigenic than the P0 line and contains cells that exhibit hallmarks of CSCs. Thus, vaccination selects for cells with stem-like properties.

Vaccination induces Nanog expression in tumor cells

Since the TC-1 P3 line had elevated levels of cells with stem-like properties, we assessed the expression of molecules associated with stemness in the P3 and P0 lines. Of the candidate molecules, only Nanog —a transcription factor pivotal in self-renewal of embryonic stem cells — showed differential expression in P3 compared to P0 cells. Nanog was upregulated nearly 10-fold in the P3 cells (Figure 2A) and was detectable in 70% of the P3 cells compared to 10% of the P0 cells (Figure 2B). To test if the induction of Nanog in the P3 line could be independent of vaccination, we applied VICE and measured Nanog mRNA levels by real-time PCR at the P0, P1, P2, and P3 stages. As a control, we performed the same analysis in N1, N2, and N3 cells generated from mice implanted with TC-1 without vaccination. Nanog mRNA levels were virtually identical in the P0, N1, N2, and N3 stages. By contrast, Nanog mRNA levels gradually increased from the P0 to the P3 stages, resulting in almost 10 times more Nanog mRNA in P3 cells than in P0 cells (Figure 3A). The frequency of cells positive for Nanog protein also increased from the P0 (15%) to P3 (80%) stages but remained at 15% in the N1 to N3 stages (Figure 3B, C). Thus, accumulation of Nanog in tumor cells is a direct consequence of vaccination.

Enhancement of the tumor stem-like phenotype by vaccination requires Nanog

Since vaccination induces Nanog expression and confers a stem-like phenotype to tumor cells, we explored whether the emergence of the stem-like phenotype required Nanog. We treated TC-1 P3 cells with siRNA targeting either Nanog (siNanog) or GFP (siGFP) and characterized their growth and stem-like properties. Compared to siGFP-treated P3 cells, siNanog-treated cells divided at less than half the rate (Figure 4A) and had less cells in S phase, decreased cyclin A expression, and increased p21 expression (Figure 4B). siNanog-treated cells also formed one-fourth the number of spheres as siGFP-treated cells (Figure 4C) and had reduced CD133 expression (Supplemental Figure 1B).

To show that Nanog directly promotes the enrichment of tumor cells with a stem-like phenotype, we retrovirally-transduced TC-1 P0 cells with DNA encoding Nanog (P0/Nanog) or empty vector (P0/no insert) and characterized their growth and stem-like features. As expected, the results from these experiments were the inverse of those from the siRNA experiments. Compared to P0/no insert cells, P0/Nanog cells divided more rapidly (Figure

4D), contained more cells in S phase, had increased cyclin A expression, and decreased p21 expression (Figure 4E). P0/Nanog cells also formed more spheres than P0/no insert cells (Figure 4F). Together these data indicate that Nanog expression confers the enhancement of the tumor stem-like phenotype of TC-1 P3 cells upon vaccination.

Nanog mediates the immune-resistant phenotype of tumor cells selected by vaccination

An increase in the frequency of CSCs following chemotherapy or radiotherapy has been documented in several types of cancer (24–26). Here we report that vaccination also selects for tumor cells resembling CSCs, and that this process is mediated by Nanog. To explore the role of Nanog in tumor immune escape, we first determined if the antigen-presenting and processing capabilities of TC-1 tumor cells were altered by Nanog expression. Nanog does not influence MHC class I or E7 protein levels after siNanog (Figure 5A, B) or Nanog delivery (Figure 5F, G) into TC-1 P3 cell or TC-1 P0 cells, respectively. Furthermore, Nanog expression in tumor cells does not affect E7 antigen presentation of TC-1 tumor cells, as the frequency of IFN-γ-secreting E7-specific CTLs was similar upon incubation with siNanog- and siGFP-treated P3 cells or Nanog- and empty vector-transduced P0 cells (Figure 5C, H). These data suggest that the resistance of P3 cells to adaptive immune surveillance is not due to changes in antigen-presentation but an intrinsic immune resistance to CTL-mediated killing. To investigate this, we treated P3 cells with either siGFP or siNanog and then mixed them with E7-specific CTLs or GrB to cause apoptosis. We measured the frequency of cells positive for the active form of caspase-3 as an index of apoptosis. After adding GrB, only 6% of siGFP-treated P3 cells underwent apoptosis, but the number increased to 60% in siNanog-treated cells (Figure 5D). Similarly, a larger degree of apoptosis was seen in siNanog-treated P3 cells mixed with E7-specific CTLs relative to siGFP-treated P3 cells mixed with E7-specific CTLs (Figure 5E). We also found significantly less P0/Nanog cells, compared to P0/no insert cells, underwent apoptosis in response to the addition of GrB (Figure 5I) or E7-specific CTLs (Figure 5J). Nanog-mediated immune escape was further confirmed by co-incubation of GFP^+ P0/no insert cells and RFP^+ P0/Nanog cells with or without E7-specific CTLs (Supplemental Figure 2). 4 times more RFP^+ P0/Nanog-RFP cells than GFP^+ P0/no insert cells survived in the presence of CTLs. Therefore, Nanog expression in tumor cells confers resistance to killing by CTLs.

We tested whether this is also the case *in vivo* by challenging mice with TC-1 P0/Nanog or P0/no insert cells followed by adoptive transfer of E7-specific CTLs or isotonic saline control. Tumor size was nearly identical in mice implanted with P0/Nanog cells regardless of whether they received adoptive therapy, indicating that the P0/Nanog cells were impervious to killing by CTLs (Figure 5K). Importantly, tumor size was similar in mice implanted with P0/Nanog cells and P0/no insert cells without adoptive therapy, demonstrating that Nanog contributes to tumorigenicity by rendering tumor cells insusceptible to immune surveillance rather than through boosting their intrinsic proliferative capacity (Figure 5K). However, tumors consistently failed to grow in mice implanted with P0/no insert cells and then subjected to adoptive therapy (Figure 5K). These findings show that Nanog expression is responsible for both the stem-like and immune-resistant phenotype acquired by tumor cells after vaccination.

Inhibition of Nanog leads to tumor control by the adaptive immune system

Because we established Nanog's central role in enhancing the tumor stem-like and immune-resistant phenotype after vaccination, we reasoned that inhibition of Nanog could control tumor progression. We challenged mice with TC-1 P3 cells. After the tumor formed, the mice received systemic injections of nanoparticles carrying siGFP or siNanog followed by adoptive transfer of CFSE-labeled, E7-specific CTLs or isotonic saline control (Figure 6A). Delivery of siNanog strongly retarded tumor growth, and the tumor was virtually eradicated

in mice given siNanog and E7-specific CTLs (Figure 6B). Mice administered siGFP had rapid tumor growth, regardless of whether they received adoptive therapy (Figure 6B). 15 days after the tumor challenge, siNanog-treated mice had tumors less than one tenth the size of tumors in siGFP-treated mice. Adoptive therapy further reduced the tumor size to one half in the siNanog-treated mice (Figure 6C). We harvested the tumors and characterized the proliferative and survival features of their component cells. siNanog-treated mice had lower levels of cyclin A and higher levels of p21 within the tumor compared to siGFP-treated mice (Figure 6D). Furthermore, only 60% of tumor cells in siNanog-treated mice were positive for Ki67, a marker of proliferation (Figure 6E). By contrast, nearly 100% of tumor cells in siGFP-treated mice were $Ki67^+$ (Figure 6E). 25% of tumor cells in siNanog-treated mice with adoptive therapy underwent apoptosis; however, the frequency was only 5% in siNanog-treated mice without adoptive therapy or in siGFP-treated mice (with or without adoptive therapy) (Figure 6G). There was no difference in the amount tumor-infiltrating transferred CTLs between siNanog- and siGFP-treated mice (Figure 6F). These results demonstrate that inhibiting Nanog restores tumor susceptibility to immunological control even after immune selection by vaccination. Interestingly, we also noted that the frequency of $CD133^+$ cells in the TC-1 P3 tumor was dropped from 64% to 36% after delivery of siNanog, indicating that Nanog inhibition impairs the enhancement of the stem-like phenotype (Supplemental Figure 1C).

Nanog confers stem-like and immune-resistant properties to human cancer cells

We also examined the presence of Nanog in human cervical cancers. Nanog was highly expressed in CUMC6 and HeLa, but not in HEK293 or CaSki cervical cancer cells (Figure 7A). We assessed the contribution of Nanog to the stem-like and immune-resistant properties of these cells. Delivery of siNanog diminished the sphere-forming capacity of $Nanog^+$ CUMC6 and HeLa cells by 5-fold (Figure 7B). siNanog-treated CUMC6 and HeLa cells were also 3 times more vulnerable to GrB-mediated apoptosis compared to siGFP-treated cells (Figure 7C). Conversely, retroviral transduction of Nanog DNA into $Nanog^-$ CaSki and HEK293 cells enhanced sphere-forming capacity by 10-fold, and 300-fold, respectively (Figure 7B). In addition Nanog-transduced CaSki or HEK293-D^b cells pulsed with $E7_{49\text{-}57}$ were 6 times more resistant to GrB- or E7-specific CTL-mediated apoptosis, respectively, compared to empty vector-transduced cells (Figure 7C, D). Thus, the presence of Nanog represents an important feature of some human cancers, promoting the gain of a stem-like and immune-resistant phenotype.

Discussion

We previously developed VICE, a system that selects for tumor immune escape variants (P3) after vaccination in a cervical cancer model (19). We found that these P3 cells impervious to lysis by tumor-reactive CTLs proliferated more rapidly in culture than the parental P0 cells from which they were derived and exhibited various hallmarks of CSCs, including sphere-forming capacity, tumor-initiating properties, and expression of pluripotency markers, including CD133, CD44, and ALDH. It is unclear whether the P3 cells are definitively CSCs. However, since the P3 cells were more pronounced in all of the above features compared to the P0 population, we conclude that P3 has been polarized towards a stem-like phenotype. Thus, in addition to chemotherapy or radiotherapy, vaccination can select for tumor cells with phenotypes resembling CSCs (27–30).

We also found that, consistent with the cancer immunoediting theory, vaccination selects for tumor cells with an immune-resistant phenotype. This phenotype could arise from either increased proliferation or survival of tumor cells (18) triggered by Nanog. Our data suggest that the immune-resistant phenotype is not likely due to a faster growth rate of the TC-1/Nanog tumor compared to the TC-1/no insert tumor because we did not observe a significant

difference in tumor progression after challenge with TC-1/Nanog or TC-1/no insert in the absence of adoptive transfer of E7-specific CD8+ CTLs (Figure 5K). It is more likely that Nanog confers an intrinsic protection from CTL-mediated killing since mice injected with TC-1/no insert, but not TC-1/Nanog, showed reduced tumor growth rates with adoptive transfer of E7-specific CTLs. This conclusion is supported by the observation that Nanog-expressing cells are impervious to CTL-mediated killing but still have similar growth rates as TC-1/no insert cells (Supplemental Figure 2).

One important concern is whether increased Nanog expression is driven in an antigen-specific manner or by inflammatory responses to vaccination. Our data indicate that Nanog expression leads to protection from antigen-specific CTL-mediated killing, resulting in the selective survival and proliferation of Nanog-expressing cells in the tumor (Figures 5E, 5J, 7D, and Supplemental Figure 2). Furthermore, *in vivo* immune selection of Nanog-expressing tumor cells was demonstrated after adoptive transfer of E7-specific CTLs (Figure 5K). Therefore, our data suggest that Nanog expression is primarily driven by immune selection mediated by antigen-specific CTLs. However, we cannot exclude the potential contribution of vaccination-induced inflammatory responses to the upregulation of Nanog.

Nanog inhibition represents an important strategy for the control of tumor growth since we found that *in vivo* knockdown of siNanog led to tumor growth retardation. This could be attributed to the repression of the CSCs considered to be essential for tumor maintenance in many solid malignancies, including cervical cancer (31). It has also been documented that elimination of CSCs can potentiate the effects of chemotherapy or radiotherapy (32–35). Thus, reduced numbers of CSCs could account for the reduction in tumor growth observed in this group of mice. Alternatively, Nanog inhibition may render tumor cells vulnerable to lysis by endogenous tumor-reactive CTLs. Either way, Nanog inhibition exerts a profound, suppressive influence on tumor growth.

The discovery that Nanog induces a stem-like and immune-resistant phenotype in cancer cells is new. This property of Nanog is not entirely surprising since Nanog is one of the core transcription factors crucial for the maintainance of self-renewal and pluripotency of embryonic stem cells (36) and for the prolonged survival of tumor cells (37). Nonetheless, little is known about the molecular mechanisms by which Nanog functions. In a recent report, Ma *et al*. demonstrated that Nanog regulates the cell cycle of embryonic stem cells via the Eras-mediated Akt pathway (38). In our previous studies, the immune-resistant phenotype of TC-1 P3 A17 tumor cells, a clone from TC-1 P3 cells, was found to depend on the pro-survival Akt kinase signaling pathway and the inhibition of apoptotic processes by up-regulation of anti-apoptotic molecules such as MCL-1, BCL-xL and BCL-2 (15, 39). The A17 tumor cells were also found to have upregulated Nanog expression (unpublished data). Further study is needed to elucidate the role of Akt signaling for the development of the stem-like and immune-resistant phenotype of TC-1/Nanog cells.

Our findings have significant implications for the development of cancer vaccination platforms. We show that Nanog-dependent emergence of a stem-like and immune-resistant phenotype in tumor cells may pose a critical barrier to current vaccination strategies., but Nanog inhibition might provide an opportunity for overcoming this barrier. Future vaccination platforms should aim to address the active tumor evolution to the immune response.

Supplementary Material

Refer to Web version on PubMed Central for supplementary material.

Acknowledgments

Financial support: This work was supported by the National Research Foundation of Korea (2009-0086652 and 2009-0076972), the Korea Healthcare Technology R&D Project (A062260), and the United States National Cancer Institute (P50 CA098252 and RO1 CA114425).

References

1. Stauss HJ. Immunotherapy with CTLs restricted by nonself MHC. Immunology Today. 1999; 20(4): 180–3. Epub 1999/04/22. [PubMed: 10203716]
2. Disis ML, Bernhard H, Jaffee EM. Use of tumour-responsive T cells as cancer treatment. Lancet. 2009; 373(9664):673–83. Epub 2009/02/24. [PubMed: 19231634]
3. Kraemer M, Hauser S, Schmidt-Wolf IG. Long-term survival of patients with metastatic renal cell carcinoma treated with pulsed dendritic cells. Anticancer Research. 2010; 30(6):2081–6. Epub 2010/07/24. [PubMed: 20651354]
4. Dillman RO, Selvan SR, Schiltz PM, McClay EF, Barth NM, DePriest C, et al. Phase II trial of dendritic cells loaded with antigens from self-renewing, proliferating autologous tumor cells as patient-specific antitumor vaccines in patients with metastatic melanoma: final report. Cancer Biotherapy & Radiopharmaceuticals. 2009; 24(3):311–9. Epub 2009/06/23. [PubMed: 19538053]
5. Lesterhuis WJ, Haanen JB, Punt CJ. Cancer immunotherapy--revisited. Nature reviews Drug Discovery. 2011; 10(8):591–600. Epub 2011/08/02.
6. Kruger C, Greten TF, Korangy F. Immune based therapies in cancer. Histology and Histopathology. 2007; 22(6):687–96. Epub 2007/03/16. [PubMed: 17357098]
7. Aptsiauri N, Carretero R, Garcia-Lora A, Real LM, Cabrera T, Garrido F. Regressing and progressing metastatic lesions: resistance to immunotherapy is predetermined by irreversible HLA class I antigen alterations. Cancer Immunology, Immunotherapy. 2008; 57(11):1727–33. Epub 2008/05/21.
8. Curiel TJ, Coukos G, Zou L, Alvarez X, Cheng P, Mottram P, et al. Specific recruitment of regulatory T cells in ovarian carcinoma fosters immune privilege and predicts reduced survival. Nature Medicine. 2004; 10(9):942–9. Epub 2004/08/24.
9. Gajewski TF. Identifying and overcoming immune resistance mechanisms in the melanoma tumor microenvironment. Clinical Cancer Research: An Official Journal of the American Association for Cancer Research. 2006; 12(7 Pt 2):2326s–30s. Epub 2006/04/13. [PubMed: 16609053]
10. Schatton T, Frank MH. Antitumor immunity and cancer stem cells. Annals of the New York Academy of Sciences. 2009; 1176:154–69. Epub 2009/10/03. [PubMed: 19796244]
11. Wilczynski JR, Duechler M. How do Tumors Actively Escape from Host Immunosurveillance? Arch Immunol Ther Ex. 2010; 58(6):435–48.
12. Han HD, Mangala LS, Lee JW, Shahzad MM, Kim HS, Shen D, et al. Targeted gene silencing using RGD-labeled chitosan nanoparticles. Clinical Cancer Research : An Official Journal of the American Association for Cancer Research. 2010; 16(15):3910–22. Epub 2010/06/12. [PubMed: 20538762]
13. Lin KY, Guarnieri FG, Staveley-O'Carroll KF, Levitsky HI, August JT, Pardoll DM, et al. Treatment of established tumors with a novel vaccine that enhances major histocompatibility class II presentation of tumor antigen. Cancer Research. 1996; 56(1):21–6. Epub 1996/01/01. [PubMed: 8548765]
14. Kang TH, Kim KW, Bae HC, Seong SY, Kim TW. Enhancement of DNA vaccine potency by antigen linkage to IFN-gamma-inducible protein-10. International Journal of Cancer. 2011; 128(3):702–14. Epub 2010/05/18.
15. Noh KH, Kang TH, Kim JH, Pai SI, Lin KY, Hung CF, et al. Activation of Akt as a mechanism for tumor immune evasion. Molecular Therapy : the Journal of the American Society of Gene Therapy. 2009; 17(3):439–47. Epub 2008/12/25. [PubMed: 19107122]
16. Chen CH, Wang TL, Hung CF, Yang Y, Young RA, Pardoll DM, et al. Enhancement of DNA vaccine potency by linkage of antigen gene to an HSP70 gene. Cancer Research. 2000; 60(4): 1035–42. Epub 2000/03/08. [PubMed: 10706121]

17. Dunn GP, Bruce AT, Ikeda H, Old LJ, Schreiber RD. Cancer immunoediting: from immunosurveillance to tumor escape. Nature Immunology. 2002; 3(11):991–8. Epub 2002/10/31. [PubMed: 12407406]
18. Schreiber RD, Old LJ, Smyth MJ. Cancer immunoediting: integrating immunity's roles in cancer suppression and promotion. Science. 2011; 331(6024):1565–70. Epub 2011/03/26. [PubMed: 21436444]
19. Wu TC. The role of vascular cell adhesion molecule-1 in tumor immune evasion. Cancer Research. 2007; 67(13):6003–6. Epub 2007/07/10. [PubMed: 17616653]
20. Wu TC, Guarnieri FG, Staveley-O'Carroll KF, Viscidi RP, Levitsky HI, Hedrick L, et al. Engineering an intracellular pathway for major histocompatibility complex class II presentation of antigens. Proceedings of the National Academy of Sciences of the United States of America. 1995; 92(25):11671–5. Epub 1995/12/05. [PubMed: 8524826]
21. Chen CH, Wang TL, Ji H, Hung CF, Pardoll DM, Cheng WF, et al. Recombinant DNA vaccines protect against tumors that are resistant to recombinant vaccinia vaccines containing the same gene. Gene Therapy. 2001; 8(2):128–38. Epub 2001/04/21. [PubMed: 11313782]
22. Frank NY, Schatton T, Frank MH. The therapeutic promise of the cancer stem cell concept. The Journal of Clinical Investigation. 2010; 120(1):41–50. Epub 2010/01/07. [PubMed: 20051635]
23. Dean M, Fojo T, Bates S. Tumour stem cells and drug resistance. Nature Reviews Cancer. 2005; 5(4):275–84. Epub 2005/04/02.
24. Du Z, Qin R, Wei C, Wang M, Shi C, Tian R, et al. Pancreatic cancer cells resistant to chemoradiotherapy rich in "stem-cell-like" tumor cells. Digestive Diseases and Sciences. 2011; 56(3):741–50. Epub 2010/08/05. [PubMed: 20683663]
25. Levina V, Marrangoni AM, DeMarco R, Gorelik E, Lokshin AE. Drug-selected human lung cancer stem cells: cytokine network, tumorigenic and metastatic properties. PLoS ONE. 2008; 3(8):e3077. Epub 2008/08/30. [PubMed: 18728788]
26. Diehn M, Clarke MF. Cancer stem cells and radiotherapy: new insights into tumor radioresistance. Journal of the National Cancer Institute. 2006; 98(24):1755–7. Epub 2006/12/21. [PubMed: 17179471]
27. Visvader JE, Lindeman GJ. Cancer stem cells in solid tumours: accumulating evidence and unresolved questions. Nature Reviews Cancer. 2008; 8(10):755–68. Epub 2008/09/12.
28. Zhou BB, Zhang H, Damelin M, Geles KG, Grindley JC, Dirks PB. Tumour-initiating cells: challenges and opportunities for anticancer drug discovery. Nature Reviews Drug Discovery. 2009; 8(10):806–23. Epub 2009/10/02.
29. Singec I, Knoth R, Meyer RP, Maciaczyk J, Volk B, Nikkhah G, et al. Defining the actual sensitivity and specificity of the neurosphere assay in stem cell biology. Nature Methods. 2006; 3(10):801–6. Epub 2006/09/23. [PubMed: 16990812]
30. Singec I, Knoth R, Meyer RP, Maciaczyk J, Volk B, Nikkhah G, et al. Defining the actual sensitivity and specificity of the neurosphere assay in stem cell biology. Nature Methods. 2006; 3(10):801–6. [PubMed: 16990812]
31. Gu W, Yeo E, McMillan N, Yu C. Silencing oncogene expression in cervical cancer stem-like cells inhibits their cell growth and self-renewal ability. Cancer Gene Therapy. 2011; 18:897–905. Epub 2011/09/10. [PubMed: 21904396]
32. Ginestier C, Liu S, Diebel ME, Korkaya H, Luo M, Brown M, et al. CXCR1 blockade selectively targets human breast cancer stem cells in vitro and in xenografts. The Journal of Clinical Investigation. 2010; 120(2):485–97. Epub 2010/01/07. [PubMed: 20051626]
33. Zielske SP, Spalding AC, Wicha MS, Lawrence TS. Ablation of breast cancer stem cells with radiation. Translational Oncology. 2011; 4(4):227–33. Epub 2011/08/02. [PubMed: 21804918]
34. Wu A, Oh S, Wiesner SM, Ericson K, Chen L, Hall WA, et al. Persistence of CD133+ cells in human and mouse glioma cell lines: detailed characterization of GL261 glioma cells with cancer stem cell-like properties. Stem Cells and Development. 2008; 17(1):173–84. Epub 2008/02/15. [PubMed: 18271701]
35. Wu Y, Wu PY. CD133 as a marker for cancer stem cells: progresses and concerns. Stem Cells and Development. 2009; 18(8):1127–34. Epub 2009/05/05. [PubMed: 19409053]

36. Yamaguchi S, Kurimoto K, Yabuta Y, Sasaki H, Nakatsuji N, et al. Conditional knockdown of Nanog induces apoptotic cell death in mouse migrating primordial germ cells. Development. 2009; 136(23):4011–20. [PubMed: 19906868]

37. Siu MK, Wong ES, Chan HY, Ngan HY, Chan KY, Cheung AN. Overexpression of NANOG in gestational trophoblastic diseases: effect on apoptosis, cell invasion, and clinical outcome. American Journal of Pathology. 2008; 173(4):1165–72. Epub 2008/07/04. [PubMed: 18772339]

38. Ma T, Wang Z, Guo Y, Pei D. The C-terminal pentapeptide of Nanog tryptophan repeat domain interacts with Nac1 and regulates stem cell proliferation but not pluripotency. The Journal of Biological Chemistry. 2009; 284(24):16071–81. Epub 2009/04/14. [PubMed: 19366700]

39. Kang TH, Noh KH, Kim JH, Bae HC, Lin KY, Monie A, et al. Ectopic expression of X-linked lymphocyte-regulated protein pM1 renders tumor cells resistant to antitumor immunity. Cancer Research. 2010; 70(8):3062–70. [PubMed: 20395201]

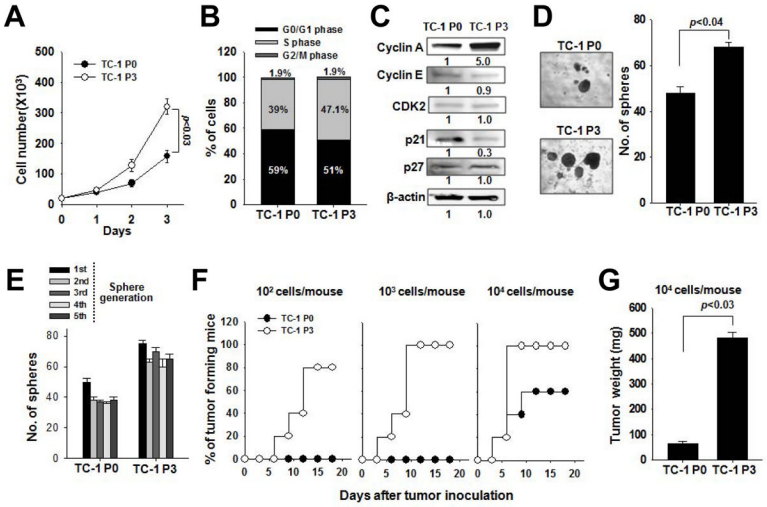

Figure 1. Growth and tumorigenicity of immune-resistant cancer cells selected by vaccination

(A) Live P0 or P3 cells were counted at each time point after trypan blue staining. (B) Cell cycle stages of cells was measured by flow cytometry. (C) Expression of cell cycle proteins was determined by Western blot from 50 μg of lysate. (D) P0 or P3 were cultured in low density suspension conditions to promote sphere formation (left). The number of spheres per well was quantified (right). (E) P0 or P3 spheres were serially passaged for 5 rounds, and the number of spheres per well was quantified at each cycle. (F) P0 or P3 cells were inoculated at different doses into NOD/SCID mice and tumor formation was monitored. (G) 18 days after challenge, tumors were explanted and weighed from the mice challenged with 10^4 cells. Data are representative of three independent experiments.

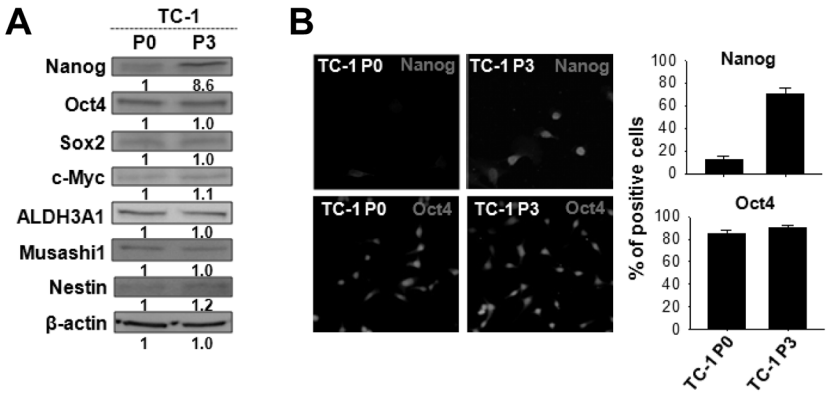

Figure 2. Expression of stemness factors in immune-resistant cancer cells selected by vaccination

(A) Expression of a panel of stemness factors was compared in P0 or P3 by Western blot. β-actin served as an internal control. (B) Nanog expression in P0 or P3 was visualized by immunofluorescence microscopy (left), and the percentage of $Nanog^+$ cells was quantified (right). Oct4 served as an internal control. Data are representative of three independent experiments.

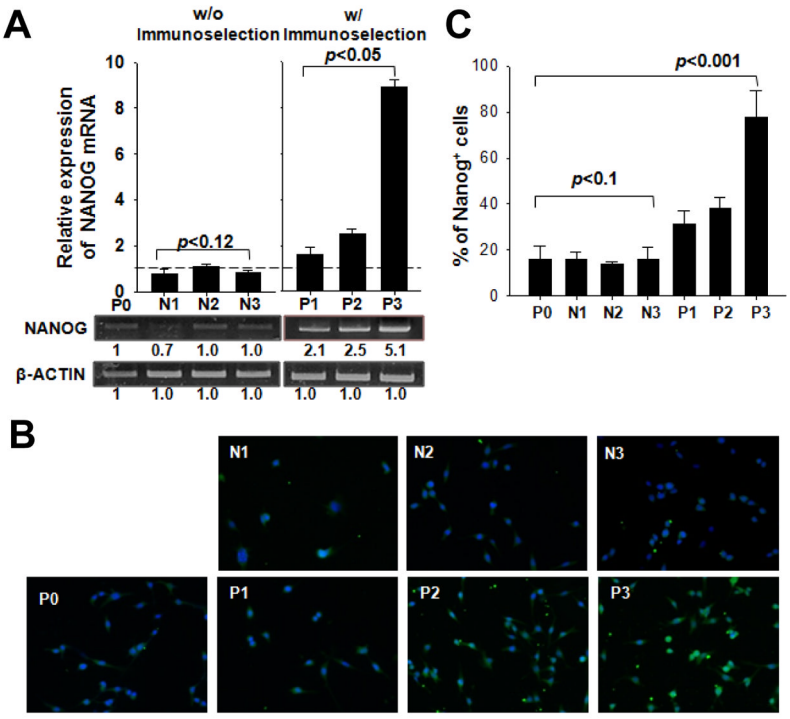

Figure 3. Accumulation of Nanog through sequential rounds of vaccination

(A) VICE was applied, and levels of Nanog mRNA were measured by real-time RT-PCR and normalized to levels of β-actin mRNA (top). Representative image of the RT-PCR end-product (bottom). (B) The frequency of Nanog$^+$ cells at each stage of immunoediting was measured by immunofluorescence analysis. (C) The percentage of Nanog$^+$ cells was quantified. Data are representative of three independent experiments.

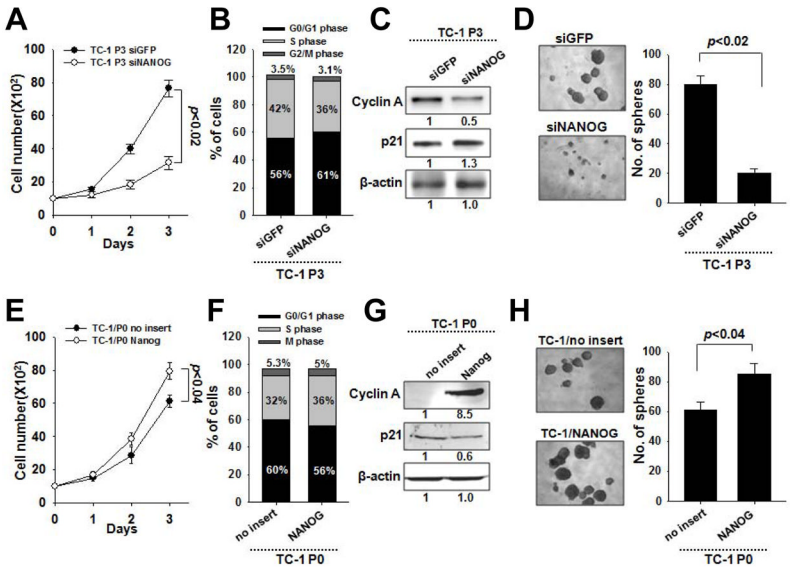

Figure 4. Contribution of Nanog to the growth and stem-like properties of immune-resistant cancer cells after vaccination

(A) live P3 cells treated with siGFP or siNanog were counted at each time point. (B) Cell cycle stages of P3 cells was measured by flow cytometry (left). The expression of various cell cycle proteins was determined (right). (C) The treated P3 cells were cultured in low density suspension conditions to promote sphere formation (left). The number of spheres per well was quantified (right). (D) The live P0 cells were counted at each time point after trypan blue staining. (E) The frequency of the transduced P0 at different cell cycle stages was measured by flow cytometry (left). The expression of various cell cycle proteins was determined (right). (F) The transduced P0 were cultured in low density suspension conditions to promote sphere formation (left). The number of spheres per well was quantified (right). Data are representative of three independent experiments.

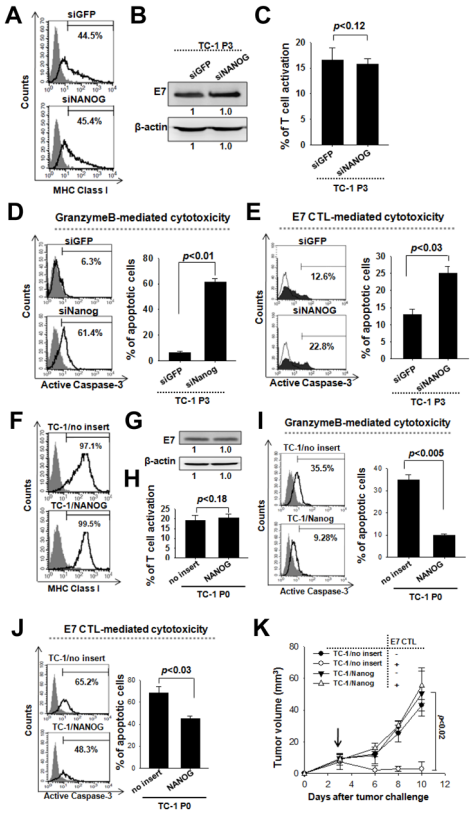

Figure 5. Role of Nanog in the immune-resistant phenotype of cancer cells selected by vaccination

(A) siGFP- or siNanog-treated P3 cells were stained with PE-labeled anti-mouse H-2D^b monoclonal antibody to detect MHC class I (black line) or isotype control (shaded region). (B) E7 protein expression in the siRNAs-treated cells was analyzed by Western blot. (C) the siRNAs-treated P3 cells were incubated with E7-specific CTLs at a 1:1 effector:target ratio for 4 hours. Cells were then stained for intracellular IFN-γ to detect CTL activation. (D) GrB was delivered into the P3 cells. The frequency of apoptotic (active caspase-3$^+$) cells was measured by flow cytometry. (E) the P3 cells were incubated with E7-specific CTLs for 4 hours at a 1:1 ratio, and the frequency of tumor cells undergoing apoptosis was assessed by staining for active caspase-3. (F) Empty vector- or Nanog-tansduced P0 cells were stained with PE-labeled anti-mouse H-2D^b antibody to detect MHC class I. (G) E7 protein expression in the transduced P0 cells. (H) The P0 cells were incubated with E7-specific CTLs and, then stained for intracellular IFN-γ to detect CTL activation. (I) GrB was delivered into the P0 cells. The frequency of caspase-3$^+$ cells was quantified after 4 hours. (J) The P0 cells were incubated with E7-specific CTLs, and The frequency of apoptotic (active caspase-3$^+$) cells was measured by flow cytometry. (K) Mice were challenged subcutaneously with 10^5 P0 cells. 3 days later, mice received adoptive transfer through the tail vein with 2×10^6 E7-specific CTLs or with isotonic saline. Data are representative of at least three independent experiments.

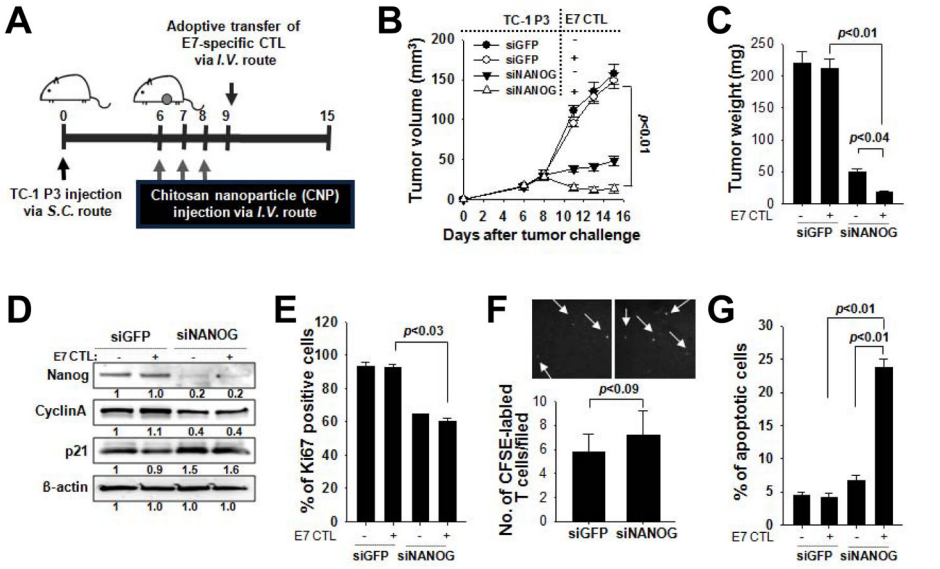

Figure 6. Control of immune-resistant tumor growth by Nanog inhibition

(A) Schematic diagram of the TC-1 P3 tumor challenge and treatment regimen. (B) Tumor growth kinetics in P3-bearing mice treated with siGFP or siNanog, without or without adoptive therapy. (C) Tumor weight in each group measured 15 days after tumor challenge. (D) Western blot to characterize expression of Nanog, cyclin A, and p21 in siGFP- or siNanog-treated P3 tumor 15 days after challenge. (E) The frequency of proliferating tumor cells was determined by flow cytometry analysis of Ki67 expression. (F) Infiltration of injected CFSE-labeled, E7-specific CTLs into the tumor was visualized by fluorescence microscopy (top) and quantified (bottom). (G) The frequency of apoptotic (active caspase-3^{+}) cells in the tumors was measured by flow cytometry. Data are representative of three independent experiments.

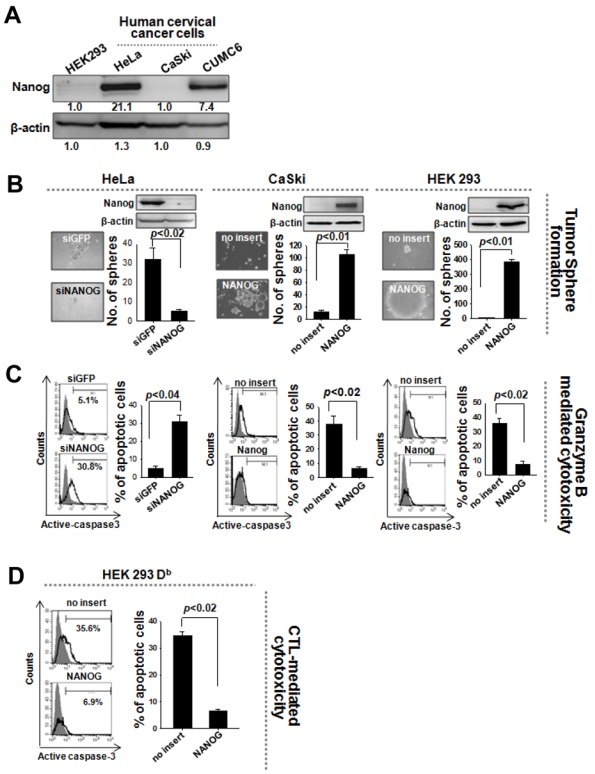

Figure 7. Nanog-mediated control of stemness and immune escape in human cancer

(A) Western blot was performed to characterize Nanog expression in human cervical cancer cells. (B) CUMC6 or HeLa cells with high levels of Nanog were treated with siGFP or siNanog. CaSki or HEK293 cells with low levels of Nanog were transduced with empty vector or NANOG. The sphere-forming capacity of these cells was analyzed in suspension culture. (C) Recombinant GrB was delivered into the cells. The frequency of apoptotic (active caspase-3^+) cells was measured by flow cytometry. (D) Empty vector- or Nanog-transduced HEK293D^b cells were pulsed with E7 peptide and then mixed with E7-specific CTLs at a 1:1 ratio. The percentage of apoptotic cells was quantified by flow cytometry. Data are representative of at least three independent experiments.